

Research report

Extracting BOLD signals based on time-constrained multiset canonical correlation analysis for brain functional network estimation and classification

Haimei Wang^{a,1}, Xiao Jiang^{a,b,1}, Renato De Leone^b, Yining Zhang^a, Lishan Qiao^a, Limei Zhang^{a,*}

^a School of Mathematics Science, Liaocheng University, Liaocheng 252000, China

^b School of Science and Technology, University of Camerino, Camerino 62032, Italy



ARTICLE INFO

Keywords:

Multiset canonical correlation analysis
Time constraint
Representative BOLD signal extraction
Brain functional network
Brain disorder classification

ABSTRACT

Brain functional network (BFN), usually estimated from blood oxygen level dependent (BOLD) functional magnetic resonance imaging (fMRI), has been proven to be a powerful tool to study the organization of the brain and discover biomarkers for diagnosis of brain disorders. Prior to BFN estimation and classification, extracting representative BOLD signals from brain regions of interest (ROIs) is a critical step. Traditional extraction methods include averaging, peaking operation and dimensionality reduction, often leading to signal cancellation and information loss. In this paper, we propose a novel method, namely time-constrained multiset canonical correlation analysis (TMCCA), to extract representative BOLD signals for subsequent BFN estimation and classification. Different from traditional methods that equally treat all BOLD signals in a ROI, the proposed method assigns weights to different BOLD signals, and learns the optimal weights to make the extracted representative signals jointly maximize the multiple correlations between ROIs. Importantly, time-constraint is incorporated into our proposed method, which can effectively encode nonlinear relationship among BOLD signals. To evaluate the effectiveness of the proposed method, the extracted BOLD signals is used to estimate BFN and, in turn, identify brain disorders, including mild cognitive impairment (MCI) and autistic spectrum disorder (ASD). Experimental results demonstrate that our proposed TMCCA can lead to better performance than traditional methods.

1. Introduction

Since the correlation of spontaneous fluctuations in blood oxygen level dependent (BOLD) signals was first observed (Biswal et al., 1995), there has been a steady increase in the interest to investigate the resting-state brain functional network (BFN). In recent years, BOLD-based BFN plays an increasingly important role in the growing field of identifying brain disorders, such as mild cognitive impairment (MCI) (Morris and Cummings, 2005; Martinez and Peplow, 2019; Li et al., 2020) and autism spectrum disorder (ASD) (Wang et al., 2019; Brieber et al., 2010; Li et al., 2017).

BOLD-based BFN can be estimated in voxel-wise and region of interest (ROI)-wise manners. For voxel-wise estimation, several classic methods have been developed, including seed-based correlation analysis (Cole et al., 2010), independent component analysis (Beckmann, 2012),

fractional amplitude of low-frequency fluctuations (Zou et al., 2008), and regional homogeneity (Zang et al., 2004). The main advantage of adopting a voxel-based method is that it takes into account the whole brain information meticulously at the mesoscopic level (Korhonen et al., 2017). However, voxel-wise BFN involves a large set of nodes, which makes brain network analysis challenging. For example, it tends to cause the curse of dimensionality, excessive computation cost and may introduce problems with collinearity (Wold et al., 1984). Besides, voxel-wise BFN lacks of interpretation in finding the potential biomarkers for identifying brain disorders. In contrast, the ROI-wise modelling methods (Tadayonnejad et al., 2014) assume that the voxels within a ROI have similar functions, and the BOLD signals of all voxels within a ROI are integrated into a representative signal of the ROI. Thus, it drastically reduces the number of nodes. In addition, compared with voxel-wise methods, the ROI-wise BFN analysis can obtain results from brain

* Corresponding author.

E-mail address: zhanglimei@lcu.edu.cn (L. Zhang).

¹ H. Wang and X. Jiang contributed equally to this work.

regions directly, so as to get a meaningful explanation. Despite its advantages, on the flip side, the ROI-wise method usually leads to a lack of robustness in the estimated functional connectivity (that is, results vary significantly due to small changes in voxel location). This is because the BOLD signals extracted from a ROI with poorly defined boundaries represents the combined signal across multiple functional areas. In fact, evaluations using simulated networks have demonstrated that even a small amount of such mixing will significantly affect all methods used for BFN estimation (Bijsterbosch et al., 2017), and, in turn, result in a severe drop in accuracy of brain disorder classification. Therefore, it is critical to adopt a robust approach to extract the representative signals from ROIs, especially when regions are poorly defined.

There are three commonly used approaches for extracting representative BOLD signal from a ROI. The first and most straightforward way is averaging all the voxel signals within the current ROI (Greicius et al., 2003). Although it is easy to implement, the averaging scheme may be distorted by non-informative or noisy signals especially on the boundary of ROI. The second approach is to generate the representative signal by determining the maximum values of all voxels in different time points within a ROI (Goncalves et al., 2001). However, the peak BOLD signal is generally biased by the selected contrast, and also sensitive to noise signals. The third approach is using principal component analysis (PCA) (Bellec, 2006), and the representative signal of each ROI is determined by the projection on the first principal component. Despite their wide applications in representative signal extraction, a common drawback of above methods is that the dependence among the time points in BOLD signals is ignored, while the signals changes dynamically over time. Besides, all these methods substantially suffer from the inaccurate boundary of brain region segmentation, and the ROIs are considered independently, thus ignoring the effects from other brain regions.

To address the above issues, in this paper we propose a novel method, namely time-constrained multiset canonical correlation analysis (TMCCA), to extract representative BOLD signals jointly from multiple ROIs. Specifically, different weights are assigned to the signals in a specific ROI based on the criterion that the extracted BOLD signal in this ROI has the greatest correlation with those in the other ROIs. Meanwhile, time constraints are incorporated into the model for capturing the dependency information that the neighbor time points in BOLD signals share the similar characteristics. As a result, TMCCA can (1) characterize nonlinear relationship among extracted representative signals from different ROIs due to the time constraints, (2) assign appropriate weights to different voxels² by jointly maximizing the correlation between multiple ROIs, and (3) extract more representative signals for further connection analysis since it has taken the relationships between ROIs into account at the stage of signal extraction.

The rest of this article is organized as follows. In Section 2, we report the experimental results on two classification tasks. In Section 3, we discuss our findings and several aspects that affect the final performance. In Section 4, we summarize the paper. Finally, in Section 5, we introduce the preprocessed data, review the most relevant studies, propose the novel representative signal extraction method (including its model and algorithm) and describe the experimental setting.

2. Results

In this section, we report the results of different methods (including Average method, Peak method, PCA, MCCA, and the proposed TMCCA) for identifying subjects with MCI/ASD from healthy controls (HCs) based on Alzheimer's Disease Neuroimaging Initiative (ADNI³) and

² For example, a possibly helpful case is that small weights are assigned to the voxels on the boundary of brain regions.

³ <http://adni.loni.ucla.edu>

Table 1

Classification results corresponding to 5 different BOLD signal extraction methods based on the BFN for ADNI and ABIDE datasets respectively.

Dataset	p-value	Method	ACC ± standard deviation	SEN ± standard deviation	SPE ± standard deviation	AUC ± standard deviation		
ADNI	p = 0.05	Average	0.8456 ± 0.0281	0.8447 ± 0.0163	0.8446 ± 0.0185	0.9311 ± 0.0128		
		Peak	0.8512 ± 0.0251	0.8555 ± 0.0182	0.8548 ± 0.0360	0.9292 ± 0.0196		
		PCA	0.7616 ± 0.0129	0.7871 ± 0.0235	0.7441 ± 0.0184	0.8994 ± 0.0152		
		MCCA	0.8460 ± 0.0123	0.8535 ± 0.0256	0.8438 ± 0.0198	0.9326 ± 0.0118		
		TMCCA	0.8512 ± 0.0223	0.8686 ± 0.0195	0.8414 ± 0.0143	0.9350 ± 0.0112		
	p = 0.01	Average	0.8212 ± 0.0152	0.8309 ± 0.0148	0.8174 ± 0.0216	0.9294 ± 0.0198		
		Peak	0.8108 ± 0.0216	0.8057 ± 0.0225	0.8180 ± 0.0208	0.9121 ± 0.0243		
		PCA	0.7584 ± 0.0198	0.7336 ± 0.0182	0.7827 ± 0.0216	0.8906 ± 0.0211		
		MCCA	0.8140 ± 0.0223	0.8122 ± 0.0156	0.8234 ± 0.0218	0.9114 ± 0.0222		
		TMCCA	0.8344 ± 0.0206	0.8580 ± 0.0209	0.8204 ± 0.0192	0.9346 ± 0.0123		
		ABIDE	p = 0.05	Average	0.6757 ± 0.0258	0.6078 ± 0.0236	0.7317 ± 0.0202	0.7546 ± 0.0198
				Peak	0.6784 ± 0.0236	0.6183 ± 0.0224	0.7460 ± 0.0281	0.7288 ± 0.0214
				PCA	0.6324 ± 0.0196	0.5378 ± 0.0234	0.7112 ± 0.0123	0.7474 ± 0.0278
				MCCA	0.6649 ± 0.0225	0.5573 ± 0.0231	0.7238 ± 0.0156	0.7292 ± 0.0197
				TMCCA	0.7081 ± 0.0199	0.6556 ± 0.0234	0.7417 ± 0.0228	0.7647 ± 0.0239
p = 0.01	Average	0.6676 ± 0.0256	0.6681 ± 0.0238	0.6693 ± 0.0196	0.7458 ± 0.0318			
	Peak	0.6351 ± 0.0236	0.5802 ± 0.0248	0.6844 ± 0.0215	0.7027 ± 0.0300			
	PCA	0.6000 ± 0.0199	0.5323 ± 0.0271	0.6713 ± 0.0158	0.5965 ± 0.0233			
	MCCA	0.6514 ± 0.0256	0.6153 ± 0.0278	0.6890 ± 0.0246	0.7339 ± 0.0248			
	TMCCA	0.6703 ± 0.0196	0.5564 ± 0.0187	0.7471 ± 0.0301	0.7554 ± 0.0299			

Autism Brain Imaging Data Exchange (ABIDE⁴) databases.

In particular, the classification results are shown in Table 1, including accuracy (ACC), sensitivity (SEN) and specificity (SPE), which are defined, respectively, as follows:

$$ACC = \frac{TP + TN}{TP + FP + TN + FN} \quad (1)$$

$$SEN = \frac{TP}{TP + FN} \quad (2)$$

$$SPE = \frac{TN}{FP + TN} \quad (3)$$

where TP indicates the number of accurately identified patients, FN indicates the number of misidentified patients. Similarly, FP and TN represent the number of HCs that are misidentified and accurately identified, respectively. It can be observed that the BOLD signals extracted by TMCCA result in BFN with the best discriminability on both

⁴ http://fcon_1000.projects.nitrc.org/indi/abide/

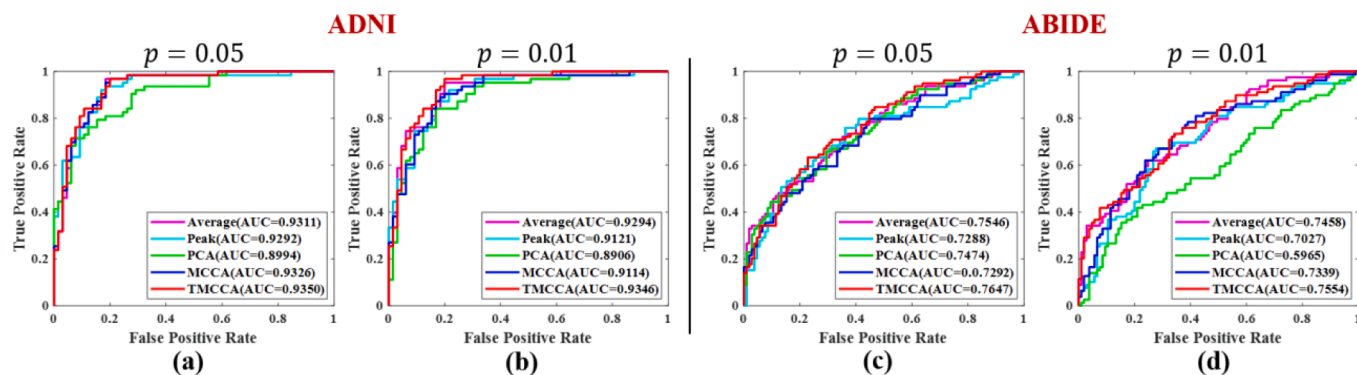


Fig. 1. The ROC curves and AUC values of TMCCA and the comparison methods: (a) 100 times 5-fold CV and $p = 0.05$ in t -test feature selection for MCI identification; (b) 100 times 5-fold CV with $p = 0.01$ in t -test feature selection for MCI identification; (c) 100 times 5-fold CV and $p = 0.05$ in t -test feature selection for ASD identification; (d) 100 times 5-fold CV with $p = 0.01$ in t -test feature selection for ASD identification.

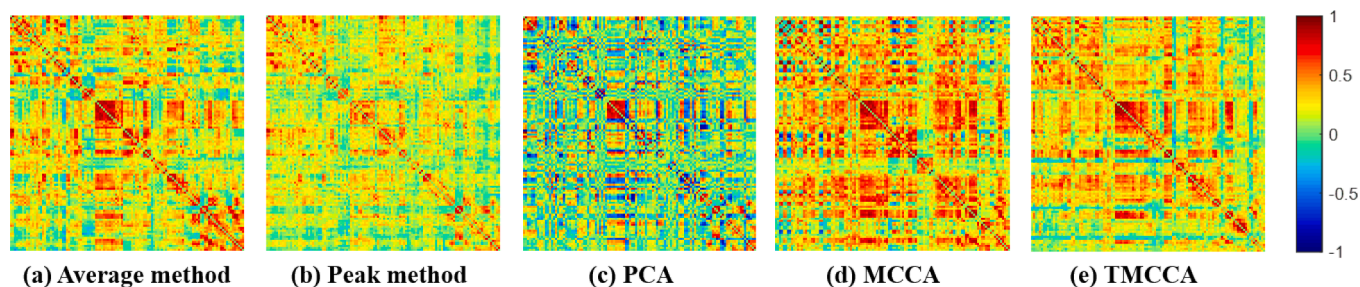


Fig. 2. The adjacency matrices (networks) of a subject. The BFNs constructed by five kind of BOLD signals using different extraction methods, including average method, peak method, PCA, MCCA, and TMCCA.

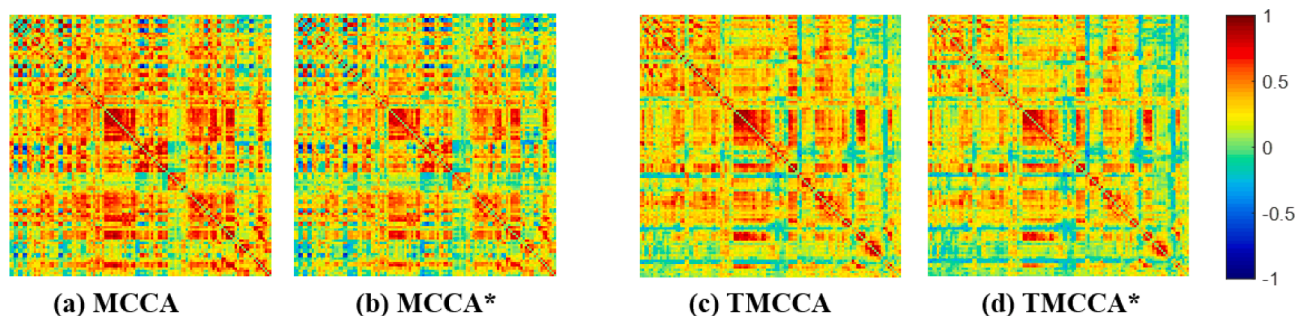


Fig. 3. The most frequently selected network connections involved in the (a) MCI identification task; (b) ASD identification task. Note that for better visual effects, the colors are randomly set. The thickness of each arc indicates the identifiability of the corresponding connection and is inversely proportional to the corresponding p -value.

ADNI and ABIDE datasets. It is also worth noting that, despite its simplicity, the averaging method performs better than the peak method, PCA and MCCA. In addition, the AUC of TMCCA outperforms the baseline methods, indicating stronger diagnostic power of the classification pipeline using TMCCA to extract signals. For the remaining indicators, the final results also show the effectiveness of the proposed method. Besides, the ROC curves of all comparison methods on both ADNI and ABIDE datasets are given in Fig. 1. It can be clearly found that the proposed method also tends to perform better than the traditional signal extraction methods.

For comparing the BFNs based on the BOLD signals extracted by five different methods, in Fig. 2 we visualize the adjacency matrices of estimated BFNs with a randomly selected subject from ADNI dataset. It can be observed that the BFN constructed based on the signals extracted by the five different methods has a similar structure and has its own characteristics at the same time. Among them, the edge weights of the BFN constructed by the peak method and PCA are relatively small. In

contrast, due to the fact that the optimization goal of MCCA is to maximize the correlation between brain regions, the edge weights of BFN based on MCCA and TMCCA are larger than those based on other baseline methods. Compared with MCCA, the edge weights of TMCCA are relatively small, because TMCCA introduces a nonlinear time similarity matrix to encode the local time information that may reduce the value of the objective function.

3. Discussion

3.1. Network connection visualization

In order to pull the BFNs associated with MCCA and TMCCA back to the same level as the other methods, we subtract the difference values of the average method matrix from all elements in the MCCA and TMCCA matrix, respectively. It can be observed from Fig. 3(b) and (d) that after subtracting the difference values between the proposed method and the

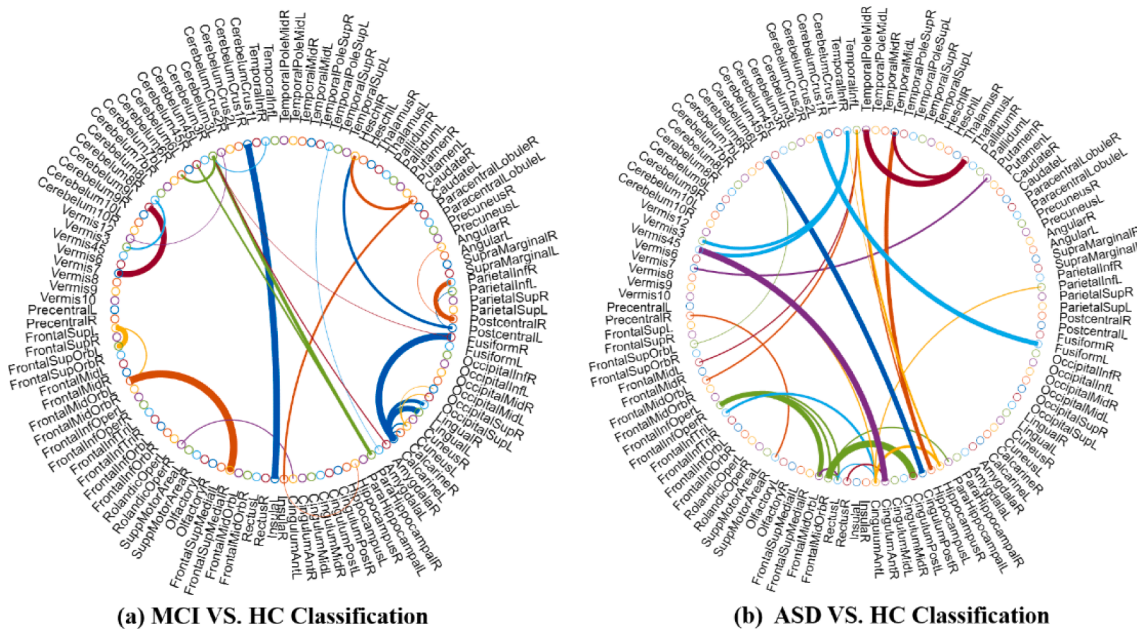


Fig. 4. The most frequently selected network connections involved in the (a) MCI identification task; (b) ASD identification task. Note that for better visual effects, the colors are randomly set. The thickness of each arc indicates the identifiability of the corresponding connection and is inversely proportional to the corresponding p -value.

average method, the network connection based on the proposed method is similar to that constructed by the average method. The reason is that TMCCA aims to maximize the correlation between multiple brain regions, which does not change the essential relationship and connection mechanism of brain regions, since we mainly care about the relative values of the edge weights.

Combined with the accuracy results shown in Table. 1, we believe that such an optimization objective of TMCCA is helpful to the subsequently constructed BFNs that may contain more discriminative connections for the identification of brain disorders.

3.2. Top discriminative features (networks connection)

As mentioned earlier, we use the estimated edge weights of BFN as classification features. In this section, we investigate the top discriminative features used to identify MCI/ASD based on our proposed TMCCA method. Specifically, we respectively select 30 and 29 connections (corresponding to the p -value of 0.0001) for identifying MCI and ASD tasks. As visualized in Fig. 4 (a), we can observe that the brain regions associated with these selected features include the right hippocampus, right caudate, right parahippocampal gyrus and right cerebellum, and bilateral amygdala, which are consistent with the brain regions selected in the previous MCI identification studies (Mckhann, et al., 2011; Anand et al., 2005; Greicius, 2008). These regions are generally believed to be the potential biomarkers for MCI/AD identification (He et al., 2007; Yetkin et al., 2006). From Fig. 4 (b), it can be found that several regions including the bilateral hippocampus, right precentral gyrus, left parahippocampal gyrus, right putamen, left middle temporal, and left middle frontal gyrus are selected in our proposed pipeline. Many of them have been reported as ASD-related brain regions in previous works (Ecker et al., 2010; Haznedar et al., 2006; Qiu et al., 2010; Rojas et al., 2006; Sparks et al., 2002; Toal et al., 2009).

3.3. Limitations and future work

Although our proposed method shows better performance in classification performance, the CCA-based algorithms are not suitable for the case that the number of voxels in a single ROI is much greater than the

number of time points. For example, some brain regions have more than 1,000 voxels, but the length of time series of the ADNI and ABIDE datasets are 135 and 175, respectively. This not only leads to a high computational cost, but also causes small-sample-size problem (Button et al., 2013), which can make the correlation between the extracted representative signals too large. To solve this problem, before using MCCA and TMCCA to extract representative signals, we first use K-means to cluster the voxels in each brain region into 10 groups according to their spatial position, and then take the average of all voxel signals in each group to reduce each brain region to 10 dimensions. In this way, the feature numbers of all brain regions can be unified, and the small-sample-size problem can be avoided since the number of features after clustering is smaller than the number of samples. However, such a scheme may result in the information loss, and the selection of clustering number (as an extra hyper-parameter) is currently an open problem. Therefore, we plan to develop a more powerful and efficient algorithm to address this problem in the future.

4. Conclusions

It is a challenging task to extract a representative BOLD signal from each ROI, due to the complex noise in data and the poorly defined boundaries of brain regions. In this paper, we propose a novel method, namely time-constrained multiset canonical correlation analysis (TMCCA), to extract the BOLD signals that can encode the temporal dynamics of ROI well. By assigning different weights to the BOLD signals in the ROIs, the proposed method tries to extract representative signals that maximize the correlation between multiple ROIs. In addition, the time constraint is used to capture the local temporal relationship among time points and model the nonlinear correlation. In order to investigate the effectiveness of the TMCCA method, we use the extracted BOLD signals to construct BFNs and then identify subjects with MCI and ASD, respectively. The experimental results demonstrate that TMCCA achieves better classification accuracy than the baseline methods.

5. Methods and materials

In this section, we describe the data preparation (including data

Table 2
Demographic information of the subjects in the ADNI and ABIDE datasets.

Dataset	Category	Gender (Male/Female)	Age (Mean + SD)
ADNI	MCI (N = 68)	39/29	72.82 ± 7.66
	HC (N = 69)	17/52	75.29 ± 5.34
ABIDE	ASD (N = 79)	68/11	14.51 ± 6.23
	HC (N = 105)	79/26	15.80 ± 3.23

subject, the fMRI data is collected over 7 min resulting in 140 brain volumes. For the ABIDE database, we use the data from New York University (NYU) site. The dataset contains 184 subjects whose demographic information is also shown in Table 2. A 3.0 T Siemens Allegra scanner was used to collect rs-fMRI images of all subjects with staring at the white gaze cross in the middle of a black background projected on the screen. For each subject, the fMRI data contain 180 brain volumes. The imaging parameters include a flip angle of 90° , 33 slices, a TR/TE of

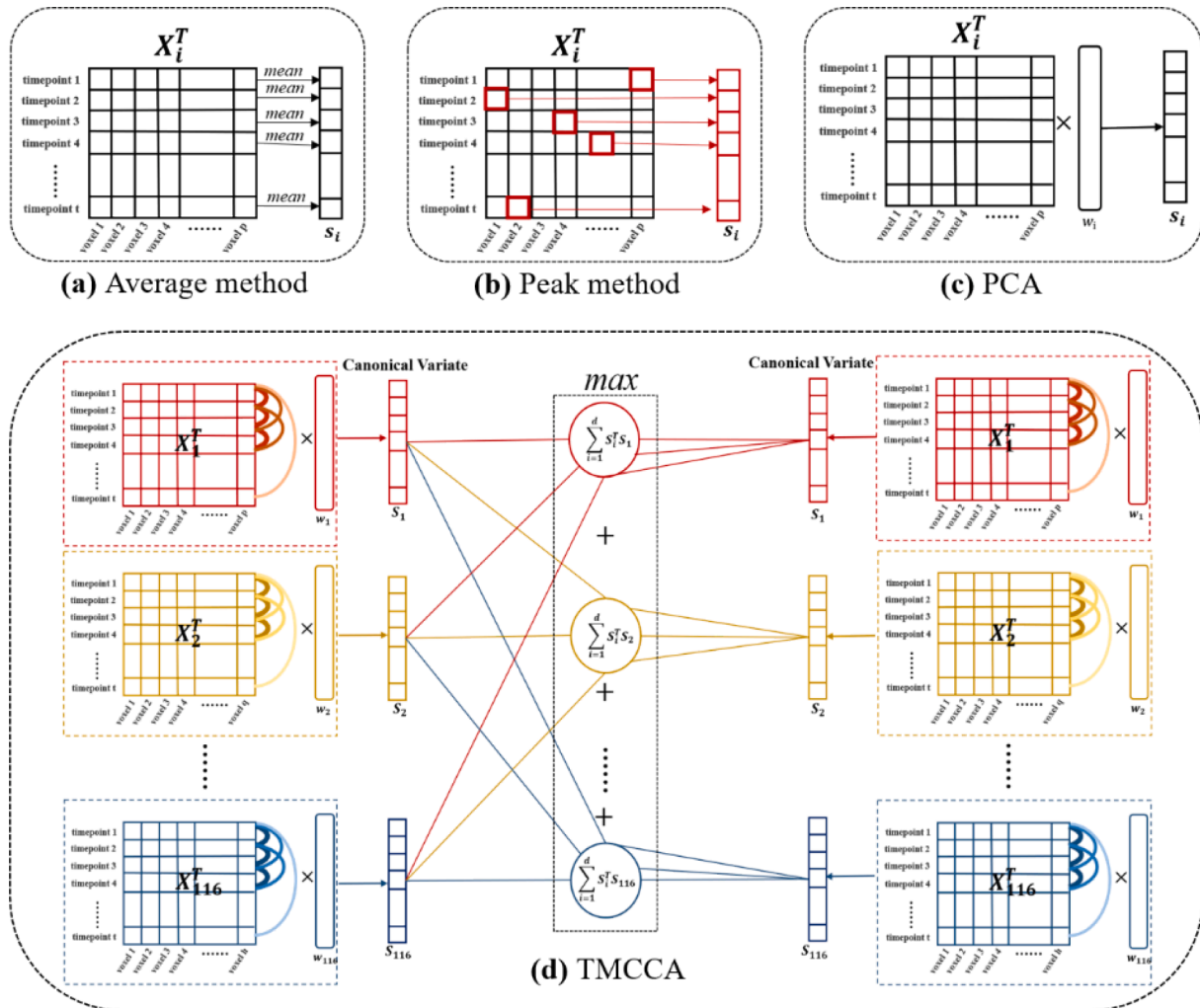


Fig. 5. Illustration of the various signal extracted methods. (a) Signal extraction mode by averaging; (b) Signal extraction mode by peak method. The signal value marked by red boxes are the maximums of the time series of each time point; (c) Signal extraction mode of PCA; (d) The working mechanism of TMCCA for representative signal extraction. This method assigns different weights to voxels by considering simultaneously two goals: 1) after projection, the ROI studied is most closely related to all the other ROIs; 2) the time series of neighbor time points are similar. Note that the thickness of each arc on the right side of the brain region data matrix represents the strength of the relationship between two timepoints.

acquisition and preprocessing), and the representative signal extraction methods (including baseline and the proposed methods).

5.1. Data acquisition and preprocessing

Two publicly available datasets, ADNI and ABIDE, are used in this study to evaluate the proposed method by identifying subjects with MCI and ASD, respectively, from HCs.

For ADNI dataset, by excluding the subjects whose head motions are larger than $2mm$ or 2° , 137 subjects were involved in our experiment. The demographics of the subjects are shown in Table 2. All subjects were scanned by 3.0 T Philips scanner with the following parameter: $TR/TE = 3000/300ms$, voxel thickness = $3.3mm$, and flip angle = 80° . For each

$2000/15ms$, and a voxel thickness of $4.0mm$.

SPM8⁵ toolbox and DPABI (Yan et al., 2016) were used to process the acquired rs-fMRI data from ADNI and ABIDE datasets. The preprocessing steps can be summarized as follows: 1) remove the first 5 volumes for signal stabilization; 2) correct volume slices and head motions; 3) regression of nuisance signals (ventricle, white matter, and head-motion with Friston 24-parameter model); 4) normalization to MNI space with resolution $3 \times 3 \times 3mm^3$; 5) spatial smooth by a kernel of $6mm$; 6) temporal filter (0.01–0.10Hz). At last, the pre-processed BOLD time

⁵ <http://www.fil.ion.ucl.ac.uk/spm/>

series signals were parcellated into 116 ROIs, according to the AAL (Tzourio-Mazoyer et al., 2002) atlas.

5.2. Related work

As discussed previously, BOLD signal extraction is a fundamental prerequisite for BFN estimation and classification. A simple and commonly-used approach to obtain the representative signals of a ROI is averaging all the signals of voxels within the ROI. Besides, peak method determines the maximum value of all signals of voxels in the ROI at each time point as the representative signal. In this section, we briefly review another frequently applied method for BOLD signal extraction from the perspective of dimensionality reduction. Then, we introduce MCCA that provides the basis for developing our model.

5.2.1. Principal component analysis

PCA is one of the most popular and simplest methods to extract the principal component of data. We suppose that each brain has been parcellated into d ROIs based on a certain atlas. The fMRI time series of voxels associated with the i th ROI is represented by $\mathbf{X}_i = [x_1^i, x_2^i, \dots, x_m^i, \dots, x_t^i] \in R^{p \times t}$, $i \in 1, \dots, d$, where p is the number of voxels in the i th ROI, and t is the number of time points in each series.

Note that we suppose that \mathbf{X}_i has been centralized, i.e., $\sum_{l=1}^p \sum_{m=1}^t x_{lm} = 0$, where x_{lm} denotes the element of the fMRI data matrix \mathbf{X}_i . Then, the projection vector \mathbf{w}_i can be calculated as follows,

$$\begin{aligned} \max_{\mathbf{w}_i} \quad & \text{tr}(\mathbf{w}_i^T \mathbf{X}_i \mathbf{X}_i^T \mathbf{w}_i) \\ \text{s.t.} \quad & \mathbf{w}_i^T \mathbf{w}_i = 1 \end{aligned} \quad (4)$$

To solve this model, the eigenvalue decomposition on the covariance matrix $\mathbf{X}_i \mathbf{X}_i^T$ can be calculated, and the projection vector \mathbf{w}_i of the i th ROI is the eigenvector corresponding to the largest eigenvalue. Finally, the representative signal of i th ROI extracted by PCA is $\mathbf{X}_i^T \mathbf{w}_i$.

5.2.2. Multiset canonical correlation analysis

MCCA (Deleus and Hulle, 2011) is a popular multivariate statistical method that can analyze the pairwise linear relationship among multiple ROIs simultaneously. Specifically, we suppose that the samples in each set conform to Gaussian distribution and have been centralized. Then, the projection matrix can be formulated as

$$(\mathbf{w}_1, \mathbf{w}_2, \dots, \mathbf{w}_d) = \arg \max_{\mathbf{w}_1, \mathbf{w}_2, \dots, \mathbf{w}_d} \frac{\sum_{i=1}^d \sum_{j=1}^d \mathbf{w}_i^T \mathbf{X}_i \mathbf{X}_j^T \mathbf{w}_j}{\sqrt{\sum_{i=1}^d \mathbf{w}_i^T \mathbf{X}_i \mathbf{X}_i^T \mathbf{w}_i}} \quad (5)$$

Equivalently, it can be further simplified to the following form:

$$\begin{aligned} \max_{\mathbf{w}_1, \mathbf{w}_2, \dots, \mathbf{w}_d} \quad & \sum_{i=1}^d \sum_{j=1}^d \mathbf{w}_i^T \mathbf{X}_i \mathbf{X}_j^T \mathbf{w}_j \\ \text{s.t.} \quad & \sum_{i=1}^d \mathbf{w}_i^T \mathbf{X}_i \mathbf{X}_i^T \mathbf{w}_i = 1 \end{aligned} \quad (6)$$

The optimization problem is equivalent to the following eigenvalue problem:

$$\begin{pmatrix} X_1 X_1^T & \dots & X_1 X_d^T \\ \vdots & \ddots & \vdots \\ X_d X_1^T & \dots & X_d X_d^T \end{pmatrix} \begin{pmatrix} \mathbf{w}_1 \\ \vdots \\ \mathbf{w}_d \end{pmatrix} = \lambda \begin{pmatrix} X_1 X_1^T & \dots & 0 \\ \vdots & \ddots & \vdots \\ 0 & \dots & X_d X_d^T \end{pmatrix} \begin{pmatrix} \mathbf{w}_1 \\ \vdots \\ \mathbf{w}_d \end{pmatrix} \quad (7)$$

where λ is a scaling factor.

5.3. The proposed method

5.3.1. Motivation

As discussed earlier, traditional BOLD signal extraction methods, such as average method and peak signal method, are generally sensitive to noise (Deleus and Hulle, 2011). In contrast, PCA for BOLD signal

extraction takes into account more information and tends to extract the signals of one ROI by discarding small eigenvalues that may correspond to the noise. However, the brain function is produced by the interactions between brain regions. Meanwhile, BOLD signals are time-dependent, and there are intrinsic nonlinear relationships among time series in a ROI. To put it simply, the representative signal extracted by the above-mentioned methods only reflect the information of the voxel signals of the studied ROI, but fails to characterize the time dependence within ROI and the potential relationship among ROIs.

Different from previous work, in this paper, we propose a new representative signal extraction method, based on the assumption that the representative signals tend to result in strong relationship among multiple brain regions. Meanwhile, the local temporal information is considered by adding time constraints according to the similar characteristics of the signals at adjacent time points. In Fig. 5, we intuitively illustrate the motivation behind the proposed model. It can be observed that the proposed method takes into account the correlation among ROIs and the relationship of neighbor time points, which can capture more information and describe the nonlinear relationships among time series. To realize the newly proposed idea, we design a model by jointly considering local temporal information and correlation among brain regions whose technical details will be described in the following section.

5.3.2. Models and algorithms

In this section, we first give an equivalent description of MCCA. Then, we introduce the local temporal constraint into MCCA, and develop the TMCCA.

The optimization problem of MCCA can be written as an equivalent description (Hoegaerts et al., 2005) as follows:

$$\begin{aligned} \min_{\mathbf{w}_1, \mathbf{w}_2, \dots, \mathbf{w}_d} \quad & \sum_{i=1}^d \sum_{j=1}^d \sum_{m=1}^t \left(\mathbf{w}_i^T (\mathbf{x}_m^i - \bar{\mathbf{x}}^i) - \mathbf{w}_j^T (\mathbf{x}_m^j - \bar{\mathbf{x}}^j) \right)^2 \\ \text{s.t.} \quad & \sum_{i=1}^d \sum_{m=1}^t \left(\mathbf{w}_i^T (\mathbf{x}_m^i - \bar{\mathbf{x}}^i) \right)^2 = 1 \end{aligned} \quad (8)$$

where $\mathbf{x}_m^i \in R^{p \times 1}$, $m \in 1, \dots, t$ is the time series of the m th time point in the i th ROI. $\mathbf{w}_i \in R^{p \times 1}$ is the weight vector whose dimension p is determined by the length of time series \mathbf{x}_m^i , and $\bar{\mathbf{x}}^i$ is the mean vector of the i th ROI. Then the objective function can be expanded as

$$\begin{aligned} \sum_{i=1}^d \sum_{j=1}^d \sum_{m=1}^t \left(\mathbf{w}_i^T (\mathbf{x}_m^i - \bar{\mathbf{x}}^i) - \mathbf{w}_j^T (\mathbf{x}_m^j - \bar{\mathbf{x}}^j) \right)^2 &= \frac{1}{2n} \sum_{i=1}^d \sum_{j=1}^d \sum_{m=1}^t \sum_{n=1}^t \left[\mathbf{w}_i^T (\mathbf{x}_m^i \right. \\ &\quad \left. - \mathbf{x}_n^i) (\mathbf{x}_m^j - \mathbf{x}_n^j)^T \mathbf{w}_j + \mathbf{w}_j^T (\mathbf{x}_m^j - \mathbf{x}_n^j) (\mathbf{x}_m^i - \mathbf{x}_n^i)^T \mathbf{w}_i \right] \\ &\quad - \frac{1}{2n} \sum_{i=1}^d \sum_{j=1}^d \sum_{m=1}^t \sum_{n=1}^t 2 \mathbf{w}_i^T (\mathbf{x}_m^i - \mathbf{x}_n^i) (\mathbf{x}_m^j - \mathbf{x}_n^j)^T \mathbf{w}_j \end{aligned} \quad (9)$$

It is easy to prove that Eq. (9) can be expressed as the following equivalent form:

$$\begin{aligned} \max_{\mathbf{w}_1, \mathbf{w}_2, \dots, \mathbf{w}_d} \quad & \sum_{i=1}^d \sum_{j=1}^d \mathbf{w}_i^T \cdot \sum_{m=1}^t \sum_{n=1}^t (\mathbf{x}_m^i - \mathbf{x}_n^i) (\mathbf{x}_m^j - \mathbf{x}_n^j)^T \cdot \mathbf{w}_j \\ \text{s.t.} \quad & \sum_{i=1}^d \mathbf{w}_i^T \cdot \sum_{m=1}^t \sum_{n=1}^t (\mathbf{x}_m^i - \mathbf{x}_n^i) (\mathbf{x}_m^i - \mathbf{x}_n^i)^T \cdot \mathbf{w}_i = 1 \end{aligned} \quad (10)$$

where the constant $1/2n$ has been ignored.

According to the definition in (Sun and Chen, 2007); \mathbf{x}_n^i can be regarded as the local neighbor of \mathbf{x}_m^i if $\|\mathbf{x}_m^i - \mathbf{x}_n^i\| \leq \varepsilon$, $i \in 1, \dots, d$, $m, n \in 1, \dots, t$, where ε is a user specified threshold. That is, the voxel signal at time point m is similar to the voxel signal at time point n . Furthermore, let $\text{LN}(\mathbf{x}_m^i)$ denote the time series that are similar to \mathbf{x}_m^i from the time points m . To introduce the time constraint that the time series signals of the neighbor time points are similar, we further define the similarity matrix $\mathbf{T}_i = \{T_{mn}^i\} \in R^{t \times t}$, $i \in 1, \dots, d$, $m, n \in 1 \dots t$. Specifically, this similarity is shown in the following way:

Table 3
Algorithm of TMCCA.

Input: $X_i = [x_1^i, x_2^i, \dots, x_m^i, \dots, x_t^i]$, $i \in 1, \dots, d$, $m \in 1, \dots, t$ -- data matrix; the threshold value ε .

Procedure:

1. Centralize all time points' voxels signals: $x_m^i \leftarrow x_m^i - \frac{1}{t} \sum_{m=1}^t x_m^i$.
2. Calculate the time constraint matrix T_{ij} by solving the Eq. (13).
3. Calculate generalized eigenvalue decomposition using Eq. (16).
4. Compute the eigenvector w corresponding to the largest eigenvalue.
5. Segment $w = \begin{pmatrix} w_1 \\ \vdots \\ w_d \end{pmatrix}$, w_i represents the weights of voxel signals in the i th brain region, whose length corresponds to the voxel length of the i th brain region.

Output: w_i -- The weight vector corresponding to the i th brain region.

$$T_{mn}^i = \begin{cases} \exp\left(-\frac{\|x_m^i - x_n^i\|^2}{t_i}\right), & \text{if } x_m^i \in LN(x_m^i) \text{ or } x_n^i \in LN(x_n^i) \\ 0, & \text{otherwise} \end{cases} \quad (11)$$

where $t_i = \sum_{m=1}^t \sum_{n=1}^t 2 \cdot \|x_m^i - x_n^i\|^2 / (t-1)$. From Eq. (11), we can observe that the more similar x_m^i and x_n^i are, the larger T_{mn}^i is. Therefore, by incorporating the local temporal constraint in MCCA, we get the final model of TMCCA as follows.

$$\begin{aligned} & \max_{w_1, w_2, \dots, w_d} \sum_{i=1}^d \sum_{j=1}^d w_i^T \cdot \sum_{m=1}^t \sum_{n=1}^t T_{mn}^i (x_m^i - x_n^i) T_{mn}^j (x_m^j - x_n^j)^T \cdot w_j \\ \text{s.t.} \quad & \sum_{i=1}^d w_i^T \cdot \sum_{m=1}^t \sum_{n=1}^t T_{mn}^i (x_m^i - x_n^i) (x_m^i - x_n^i)^T \cdot w_i = 1 \end{aligned} \quad (12)$$

Further, after a series of simple algebraic operations, the optimization problem in Eq. (12) can be rewritten as:

$$\begin{aligned} & \max_{w_1, w_2, \dots, w_d} \sum_{i=1}^d \sum_{j=1}^d w_i^T X_i T_{ij} X_j^T w_j \\ \text{s.t.} \quad & \sum_{i=1}^d w_i^T X_i T_{ii} X_i^T w_i = 1 \end{aligned} \quad (13)$$

where, $T_{ij} = D_{ij} - T_i^\circ T_j^\circ$, $i, j \in 1, \dots, d$, is a symmetric matrix. We define that the sign $^\circ$ represents an operator $(T_i^\circ T_j)_{mn} = T_{mn}^i T_{mn}^j$, $(T_i^\circ T_j) \in R^{t \times t}$. $D_{ij} \in R^{t \times t}$ is a diagonal matrix, the element on its i th diagonal element is the sum of the elements in the i th row (or the i th column due to symmetry) of the matrix $T_i^\circ T_j$.

Equivalently, Eq. (13) can be transformed to the following formula by Lagrange multiplier method:

$$Lw_1, w_2, \dots, w_d = \sum_{i=1}^d \sum_{j=1}^d w_i^T X_i T_{ij} X_j^T w_j - \lambda \left(\sum_{i=1}^d w_i^T X_i T_{ii} X_i^T w_i - 1 \right) \quad (14)$$

Let $\frac{\partial L}{\partial w_i} = 0$, $i \in 1, \dots, d$, Eq. (14) can be expressed as

$$\sum_{j=1}^d X_i T_{ij} X_j^T w_j = \lambda X_i T_{ii} X_i^T w_i \quad (15)$$

Similar to the derivation of Eq. (7), Eq. (15) can be written as

$$\begin{pmatrix} X_1 T_{11} X_1^T & \dots & X_1 T_{1d} X_d^T \\ \vdots & \ddots & \vdots \\ X_d T_{d1} X_1^T & \dots & X_d T_{dd} X_d^T \end{pmatrix} \begin{pmatrix} w_1 \\ \vdots \\ w_d \end{pmatrix} = \lambda \begin{pmatrix} X_1 T_{11} X_1^T & \dots & 0 \\ \vdots & \ddots & \vdots \\ 0 & \dots & X_d T_{dd} X_d^T \end{pmatrix} \begin{pmatrix} w_1 \\ \vdots \\ w_d \end{pmatrix} \quad (16)$$

Thus, our method is transformed into a generalized eigenvalue problem. Finally, we summarize the algorithm for solving Eq. (16) in Table 3.

5.4. Estimating BFN

Once we obtain the representative signals for all ROIs, the subsequent task is to build the BFN. In practice, many methods have been proposed to estimate the BFN for brain disorder identification (Smith et al., 2013; Lee et al., 2011; Qiao et al., 2016; Jiang et al., 2019; Li et al., 2019). In this study, Pearson's correlation (PC), is employed to construct BFN, due to its simplicity and popularity.

5.5. Feature selection and classification

In this study, we use edge weights of BFN as the features for MCI/ASD recognition. As described above, the preprocessed data is parcellated into 116 brain regions, and so the symmetric BFN adjacency matrix will generate $116 \times (116 - 1) / 2 = 6670$ edges, which is much larger than the sample size and may lead to the curse of dimensionality. Therefore, prior to the classification task, we use t -test with empirical p -value (0.05 and 0.01) to filter out low discriminative features. When the features with high discriminative power are selected, linear support vector machine (SVM) (Chang and Lin, 2011) with the default parameter (*i.e.*; $C = 1$) is employed for brain disorders classification. Note that the SVM classifier can be efficiently trained using the LIBSVM toolbox. In our experiments, to verify the stability of the proposed method, we used 100 times 5-fold cross validation (5-fold CV) to evaluate the final

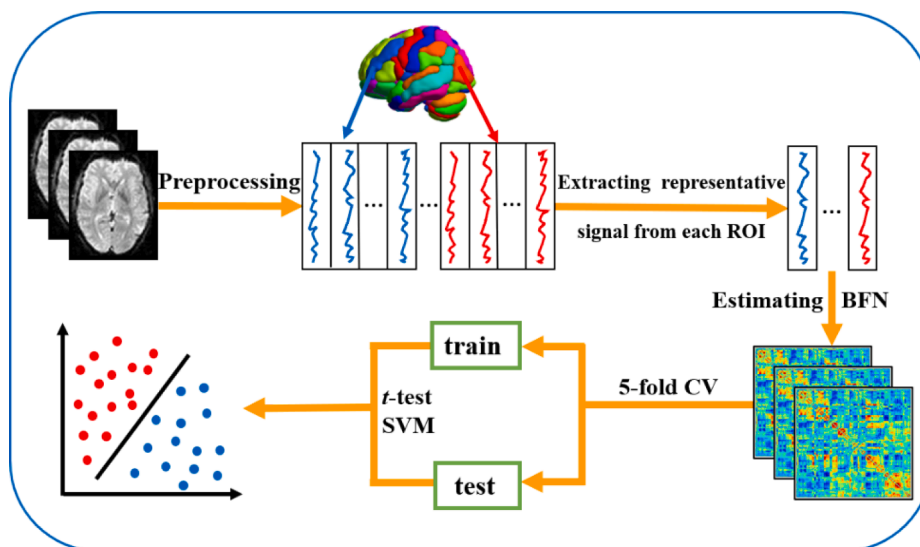


Fig. 6. The MCI/ASD identification pipeline based on the estimated BFNs.

classification performance (Rodriguez et al., 2010). Specifically, a summary of the involved brain disorders classification framework is shown in Fig. 6.

CRediT authorship contribution statement

Haimei Wang: Data curation, Writing – original draft. **Xiao Jiang:** Visualization, Investigation, Validation. **Renato De Leone:** Supervision. **Yining Zhang:** Software. **Lishan Qiao:** Writing – review & editing. **Limei Zhang:** Conceptualization, Methodology.

References

- Anand, A., et al., 2005. Activity and connectivity of brain mood regulating circuit in depression: a functional magnetic resonance study. *Biol. Psychiatry* 57 (10), 1079–1088.
- Beckmann, C.F., 2012. Modelling with independent components. *NeuroImage* 62 (2), 891–901.
- Bellec, P., et al., 2006. Identification of large-scale networks in the brain using fMRI. *NeuroImage* 29 (4), 1231–1243.
- Bijsterbosch, J., Smith, S. M., Beckmann, C. F., 2017, “An Introduction to Resting State fMRI Functional Connectivity;”.
- Biswal, B., Yetkin, F.Z., Haughton, V.M., Hyde, J.S., 1995. Functional connectivity in the motor cortex of resting human brain using echo-planar MRI. *Magn. Reson. Med.* 34 (4), 537–541.
- Brieber, S., Herpertz-Dahlmann, B., Fink, G.R., Kamp-Becker, I., Remschmidt, H., Konrad, K., 2010. Coherent motion processing in autism spectrum disorder (ASD): an fMRI study. *Neuropsychologia* 48 (6), 1644–1651.
- Button, K.S., et al., 2013. Power failure: why small sample size undermines the reliability of neuroscience. *Nat. Rev. Neurosci.* 14, 365–376.
- Chang, C., Lin, C., 2011. LIBSVM: A library for support vector machines. *ACM Trans. Intell. Syst. Technol.* 2 (3), 1–27.
- Cole, D.M., Smith, S.M., Beckmann, C.F., 2010. Advances and pitfalls in the analysis and interpretation of resting-state FMRI data. *Front. Syst. Neurosci.* 4 (8), 8.
- Deleus, F., Hulle, M.M.V., 2011. Functional connectivity analysis of fMRI data based on regularized multiset canonical correlation analysis. *J. Neurosci. Methods* 197 (1), 143–157.
- Ecker, C., et al., 2010. Investigating the predictive value of whole-brain structural MR scans in autism: A pattern classification approach. *NeuroImage* 49 (1), 44–56.
- Goncalves, M.S., Hall, D.A., Johnsrude, I.S., Haggard, M.P., 2001. Can meaningful effective connectivities be obtained between auditory cortical regions? *NeuroImage* 14 (6), 1353–1360.
- Greicius, M., 2008. Resting-state functional connectivity in neuropsychiatric disorders. *Curr. Opin. Neurol.* 21 (4), 424–430.
- Greicius, M.D., Krasnow, B., Reiss, A.L., Menon, V., 2003. Functional connectivity in the resting brain: a network analysis of the default mode hypothesis. *PNAS* 100 (1), 253–258.
- Haznedar, M.M., Buchsbaum, M.S., Hazlett, E.A., Licalzi, E.M., Cartwright, C., Hollander, E., 2006. Volumetric analysis and three-dimensional glucose metabolic mapping of the striatum and thalamus in patients with autism spectrum disorders. *Am. J. Psychiatry* 163 (7), 1252–1263.
- He, Y., et al., 2007. Regional coherence changes in the early stages of Alzheimer’s disease: a combined structural and resting-state functional MRI study. *NeuroImage* 35 (2), 488–500.
- Hoegaerts, L., Suykens, J.A.K., Vandewalle, J., Moor, B.D., 2005. Subset based least squares subspace regression in RKHS. *Neurocomputing* 63, 293–323.
- Jiang, X., Zhang, L., Qiao, L., Shen, D., 2019. Estimating functional connectivity networks via low-rank tensor approximation with applications to MCI identification. *IEEE Trans. Biomed. Eng.* 67 (7), 1912–1920.
- Korhonen, O., Saarimäki, H., Glerean, E., Sams, M., Saramäki, J., 2017. Consistency of Regions of Interest as nodes of fMRI functional brain networks. *Network Neurosci.* 1 (3), 254–274.
- Lee, H., Lee, D.S., Kang, H., Kim, B., Chung, M.K., 2011. Sparse brain network recovery under compressed sensing. *IEEE Trans. Med. Imaging* 30 (5), 1154–1165.
- Li, W., Wang, Z., Zhang, L., Qiao, L., Shen, D., 2017. Remodeling Pearson’s correlation for functional brain network estimation and autism spectrum disorder identification. *Front. Neuroinf.* 11, 55.
- Li, W., Zhang, L., Qiao, L., Shen, D., 2019. Toward a better estimation of functional brain network for mild cognitive impairment identification: a transfer learning view. *IEEE J. Biomed. Health. Inf.* 24 (4), 1160–1168.
- Li, W., Xu, X., Gao, X., Wang, P., 2020. Multiple connection pattern combination for mild cognitive impairment identification from single modal data. *IFAC-PapersOnLine* 53 (5), 7–12.
- Martinez, B., Peplow, P.V., 2019. MicroRNAs as diagnostic and therapeutic tools for Alzheimer’s disease: advances and limitations. *Neural Regen. Res.* 14 (2), 242–255.
- G. M. Mckhann et al., 2011, “The diagnosis of mild cognitive impairment due to Alzheimer’s disease: recommendations from the National Institute on Aging-Alzheimer’s Association workgroups on diagnostic guidelines for Alzheimer’s disease,” *Alzheimer’s & Dementia*, 7(3).
- Morris, J.C., Cummings, J., 2005. Mild cognitive impairment (MCI) represents early-stage Alzheimer’s disease. *J. Alzheimers Dis.* 7 (3), 235–239.
- Qiao, L., Zhang, H., Kim, M., Teng, S., Zhang, L., Shen, D., 2016. Estimating functional brain networks by incorporating a modularity prior. *NeuroImage* 141, 399–407.
- Qiu, A., Adler, M., Crocetti, D., Miller, M.I., Mostofsky, S.H., 2010. Basal Ganglia Shapes Predict Social, Communication, and Motor Dysfunctions in Boys With Autism Spectrum Disorder. *J. Am. Acad. Child Adolesc. Psychiatry* 49 (6), 539–551.e4.
- Rodriguez, J.D., Perez, A., Lozano, J.A., 2010. Sensitivity analysis of k-fold cross validation in prediction error estimation. *IEEE Trans. Pattern Anal. Mach. Intell.* 32 (3), 569–575.
- Rojas, D.C., Peterson, E., Winterrowd, E., Reite, M.L., Rogers, S.J., Tregellas, J.R., 2006. Regional gray matter volumetric changes in autism associated with social and repetitive behavior symptoms. *BMC Psychiatry* 6 (1).
- Smith, S.M., et al., 2013. Functional connectomics from resting-state fMRI. *Trends Cognit. Sci.* 17 (12), 666–682.
- Sparks, B.F., et al., 2002. Brain structural abnormalities in young children with autism spectrum disorder. *Neurology* 59 (2), 184–192.
- Sun, T., Chen, S., 2007. Locality preserving CCA with applications to data visualization and pose estimation. *Image Vis. Comput.* 25 (5), 531–543.
- Tadayonnejad, R., Yang, S., Kumar, A., Ajilore, O., 2014. Multimodal brain connectivity analysis in unmedicated late-life depression. *PLoS ONE* 9 (4), e96033.
- Toal, F., et al., 2009. Psychosis and autism: magnetic resonance imaging study of brain anatomy. *Br. J. Psychiatry* 102 (5), 418–425.
- Tzourio-Mazoyer, N., et al., 2002. Automated anatomical labeling of activations in SPM using a macroscopic anatomical parcellation of the MNI MRI single-subject brain. *NeuroImage* 15 (1), 273–289.
- Wang, M., Zhang, D., Huang, J., Yap, P.T., Liu, M., 2019. Identifying autism spectrum disorder with multi-site fMRI via low-rank domain adaptation. *IEEE Trans. Med. Imaging* 39 (3), 644–655.
- Wold, S., Ruhe, A., Wold, H., Dunn, W.J., 1984. The collinearity problem in linear regression. The Partial Least Squares (PLS) approach to generalized inverses. *Siam J. Sci. Statistical Comput.* 5 (3), 735–743.
- Yan, C., Wang, X., Zuo, X., Zang, Y., 2016. DPABI: Data Processing & Analysis for (Resting-State) Brain Imaging. *Neuroinformatics* 14 (3), 339–351.
- Yetkin, F.Z., Rosenberg, R.N., Weiner, M.F., Purdy, P.D., Cullum, C.M., 2006. FMRI of working memory in patients with mild cognitive impairment and probable Alzheimer’s disease. *Eur. Radiol.* 16 (1), 193–206.
- Zang, Y., Jiang, T., Lu, Y., He, Y., Tian, L., 2004. Regional homogeneity approach to fMRI data analysis. *NeuroImage* 22 (1), 394–400.
- Zou, Q., et al., 2008. An improved approach to detection of amplitude of low-frequency fluctuation (ALFF) for resting-state fMRI: fractional ALFF. *J. Neurosci. Methods* 172 (1), 137–141.